



The image quality and diagnostic performance of CT perfusion-derived CT angiography versus that of conventional CT angiography

Xiu-Zhi Zhou^{1#}, Kuan Lu^{1#}, Du-Chang Zhai¹, Man-Man Cui¹, Yan Liu¹, Ting-Ting Wang¹, Dai Shi¹, Guo-Hua Fan¹, Sheng-Hong Ju², Wu Cai¹

¹Department of Radiology, The Second Affiliated Hospital of Soochow University, Suzhou, China; ²Department of Radiology, Zhongda Hospital, Medical School of Southeast University, Nanjing, China

Contributions: (I) Conception and design: D Shi; (II) Administrative support: W Cai; (III) Provision of study materials or patients: K Lu; (IV) Collection and assembly of data: XZ Zhou; (V) Data analysis and interpretation: XZ Zhou, K Lu; (VI) Manuscript writing: All authors; (VII) Final approval of manuscript: All authors.

[#]These authors contributed equally to this work.

Correspondence to: Wu Cai, PhD; Dai Shi, MD. Department of Radiology, The Second Affiliated Hospital of Soochow University, 1055 Sanxiang Road, Gusu District, Suzhou 215004, China. Email: xwg608@126.com; shidai1987@foxmail.com.

Background: The combination of computed tomography angiography (CTA) and computed tomography perfusion (CTP) evaluation of cerebral perfusion status and vascular conditions can improve the diagnostic accuracy of infarction, ischemia, and vascular occlusion in stroke patients, as well as a comprehensive assessment of cerebral edema, collateral circulation, and blood perfusion in the lesion area. However, the consequent radiation safety and contrast agent nephropathy have aroused increasing concern. The purpose of this study was to assess the image quality and diagnostic accuracy of CTA images derived from CTP data, and to explore the feasibility of replacing conventional CTA.

Methods: A total of 31 consecutive patients with suspected acute ischemic stroke were retrospectively analyzed. All patients underwent head and neck CTA and brain CTP examinations. All the CTP images were transmitted to the ShuKun artificial intelligence system, which reconstructs CTA derived from CTP (CTA-DF-CTP). The images were divided into 2 groups, including CTA-DF-CTP (Group A) and conventional CTA (Group B). The CT attenuation values, subjective image noise, signal-to-noise ratio (SNR), contrast-to-noise ratio (CNR), image quality, CT volume dose index (CTDI_{vol}), dose length product (DLP), and effective radiation dose (ED) were compared between the 2 groups. Moreover, the consistency of vascular stenosis and stenosis degree between the 2 groups were measured and evaluated.

Results: There were no significant differences in image noise, SNR, or CNR between Groups A and B ($P > 0.05$). The CT attenuation values of the arteries were higher in Group A than in B [internal carotid artery (ICA) = 548 ± 112 vs. 454 ± 85 Hounsfield units (HU), middle cerebral artery (MCA) = 453 ± 118 vs. 388 ± 70 HU, and basilar artery (BA) = 431 ± 99 vs. 360 ± 83 HU] ($P < 0.01$). The image quality of the 2 groups met the requirement of clinical diagnosis (4.97 ± 0.18 vs. 4.94 ± 0.25). No significant difference was found in subjective evaluation ($P > 0.05$). In Group A compared with Group B, the following reductions were observed: CTDI_{vol} (10.7%; 100.8 vs. 112.9 mGy), DLP (23.0%; $1,613 \pm 0$ vs. $2,093 \pm 88$ mGy-cm), and ED (23.0%; 5.00 ± 0.00 vs. 6.49 ± 0.27 mSv).

Conclusions: CTA-DF-CTP data provide diagnostic accuracy and image quality similar to those of conventional CTA of head and neck CTA.

Keywords: Computed tomography angiography (CTA); computed tomography perfusion (CTP); diagnostic accuracy; image quality

Submitted Sep 19, 2022. Accepted for publication Jul 07, 2023. Published online Jul 20, 2023.

doi: 10.21037/qims-22-988

View this article at: <https://dx.doi.org/10.21037/qims-22-988>

Introduction

Ischemic stroke is the most common form of stroke and is characterized by brain tissue damage caused by occlusion of cerebral arteries and cerebral circulation insufficiency (1). Ischemic stroke is considered one of the major fatal diseases in the world, with high morbidity, mortality, disability, and recurrence rates (2). Clinical studies have shown that intravenous thrombolytic therapy within 4.5 hours or mechanical thrombectomy within 6 hours of the onset of stroke can reduce the scope of cerebral infarction and greatly reduce complications (2,3). Therefore, early detection, early diagnosis, and targeted treatment are of great significance to rescue patients' lives and restore their normal functions.

Cerebral computed tomography (CT) angiography (CTA) is the standard method for the evaluation of vascular stenosis in the diagnosis of acute stroke, which can detect vascular occlusive thrombi, atherosclerotic plaques, or vascular malformations (4). CT perfusion (CTP) can reflect changes in the perfusion volume of organs on the time axis, which can not only evaluate the penumbra and infarct core volume of cerebral ischemic stroke patients, but also quantitatively evaluate tertiary cerebral collateral circulation from the perfusion level (5). Several studies have reported that the multimodal CT evaluation of cerebral perfusion status and vascular conditions, such as the combination of unenhanced CT with CTP and CTA, can improve the diagnostic accuracy of infarction, ischemia, and vascular occlusion in stroke patients (6,7), as well as a comprehensive assessment of cerebral edema, collateral circulation, and blood perfusion in the lesion area (5). However, the consequent radiation safety and contrast agent nephropathy have aroused increasing concern (8,9).

Previous studies have demonstrated that CTA can be derived from CTP data (10). CTP images and data also contain information about the vasculature. This information is extracted and presented as a dynamic angiography sequence, referred to as dynamic CTA or 4-dimensional (4D)-CTA. In addition, a high-quality 3-dimensional (3D)-CTA dataset can be reconstructed from the 4D-CTA data by showing the maximum contrast enhancement over time during the CTP process (10). Provided that the images of CTA derived from CTP

(CTA-DF-CTP) have excellent image quality, the CTA scan can be omitted. This method can reduce the radiation dose and contrast agent iodine intake by reducing the total scan time and iodine contrast agent injection volume, which can improve the safety of patients.

In this study, we aimed to evaluate the image quality and diagnostic performance of CTA-DF-CTP and to explore the feasibility of replacing conventional CTA with this technology.

Methods

Population

The study was conducted in accordance with the Declaration of Helsinki (as revised in 2013). The study was approved by the institutional ethics committee board of The Second Affiliated Hospital of Soochow University and informed consent was provided by all participants.

A total of 31 patients from December 2021 to February 2022 who were clinically suspected of having cerebral vascular disease were enrolled in the study. The exclusion criteria were as follows: iodine contrast agent allergy, surgical history of stent implantation and aneurysm clipping or embolization, motion artifacts, or severe heart, liver, and renal insufficiency. All 31 patients (23 males and 8 females) had undergone head and neck CTA and CTP and were distributed into Group A (n=31; CTA-DF-CTP) and Group B (n=31; conventional CTA). The average age was 67.07 ± 13.42 years, ranging from 31 to 91 years.

CTA and CTP protocol

All participants underwent a CTP and conventional CTA examination. The imaging studies were performed using a 256-multidetector CT system (Brilliance iCT, Philips Healthcare, Cleveland, OH, USA). For the CTP scan, 40 mL of contrast material (370 mg iodine/mL; Ultravist 370, Bayer Schering Pharma, Berlin, Germany) was injected into the cubital vein using an 18 G needle at a rate of 5 mL/s followed by a 30 mL saline flush at a rate of 5 mL/s using a high-pressure syringe (MissouriXD2001, Ulrich, Ulm, Germany). The CTP scanning was performed with the toggling table technique (Jog mode) during a

total scanning time of 56 seconds and the parameters were 80 kVp, 180 mAs, 128×0.625 mm collimation, and 512×512 matrix. The CTP scanning was executed 4 seconds after the initiation of contrast medium injection, the scanning interval was 4 seconds for each circle, and a total of 14 scans were performed, with the scanning range of 160 mm from the skull base to the vertex, consisting of 32 slices at 5 mm thickness (total of 448 images). For CTA, another 40 mL of contrast material was injected at a rate of 5 mL/s, followed by 30 mL saline flush at a rate of 5 mL/s. The CTA scanning parameters were 100 kVp, 150 mAs, 128×0.625 mm collimation, 512×512 matrix, 0.9 mm slice thickness, and the scanning range of 373±22 mm from the aortic arch to the vertex. The start time of data acquisition was determined with a computer-assisted bolus-tracing program (Bolus Tracking; Philips Healthcare) with a trigger threshold of 120 Hounsfield units (HU) in the aortic arch, and data acquisition started 2.5 seconds after triggering. Volume rendering (VR) and conventional maximum intensity projection (MIP) postprocessing were performed on a multimodality workstation (Philips Medical Systems, Philips Healthcare, Best, The Netherlands) or an artificial intelligence reconstruction system (ShuKun application, Beijing, China) for each patient.

CTA-DF-CTP reconstruction

The ShuKun artificial intelligence reconstruction system was used to reconstruct CTA images derived from CTP. CTA-DF-CTP consists of 160 slices at 1 mm thickness. The algorithm of CTA-DF-CTP mainly includes 2 parts: single CTP phase selection and CTA reconstruction. CTA-DF-CTP of ShuKun application is based on the imaging principle of CTP, in which the CT value of brain tissue will gradually rise to the peak value and then gradually decline to the bolus tail with time after the injection of contrast agent. First, the anterior cerebral artery (ACA), middle cerebral artery (MCA), and basilar artery (BA) in CTP images were segmented using a deep learning algorithm to obtain the corresponding arterial vessels. Then, the time-density curve (TDC) of each arterial point pair was analyzed, the characteristics of the line curve were analyzed combined with clinical knowledge, and only 1 TDC was selected for the next perfusion process. The TDC selected was also used to select the single CTP phase to reconstruct CTA. The single CTP phase with the highest CT value in the TDC was selected. The reconstruction algorithm

comprised almost the same process of standard CTA images, which is first vessel segmentation using deep learning to obtain a cerebral vascular mask on the selected CTP single phase images. Although the image quality of CTP is always lower than that of standard CTA images, the deep learning algorithm can deal with this segmentation task well. The VR algorithm in CTA can be processed on these masks. Then, some centerline extraction and vessel name identify methods were applied to generate curve planar reformation (CPR) images. Conventional MIP postprocessing was applied to generate MIP images.

Objective image quality evaluation

A professional radiologist with 5 years of CTA experience measured and compared 2 sets of CTA images. Vascular attenuation (HU) was measured with a circular region of interest (ROI), placed in the center of the vessels at the following sites: bilateral internal carotid artery (ICA), bilateral MCA, M1 segment, and BA. All ROIs (range, 3–7 mm²) were placed in the enhanced lumen of the vessels, avoiding inclusion of other structures such as the edges of vessels, atherosclerotic plaques, and calcifications. The background signal was measured with a circular ROI (range, 5–10 mm²), which was placed at the bilateral temporal muscle at the same slice as the artery. The standard deviation (SD) of vascular attenuation was deemed image noise. The signal-to-noise ratio (SNR) and contrast-to-noise ratio (CNR) were calculated for all patients based on the following formulas: $SNR = HU_{\text{vessel}}/SD_{\text{vessel}}$ and $CNR = (HU_{\text{vessel}} - HU_{\text{muscle}})/SD_{\text{vessel}}$ (8,11). Target areas were made as consistent as possible in the same level of the 2 groups of CTA.

Partial head and neck arteries were selected for each patient: bilateral external carotid artery (ECA), bilateral ICA, and bilateral vertebral artery (VA). The stenosis rate of the vessels was evaluated for all patients using the following formulas: $\text{stenosis rate} = (1 - D_s/D_n) \times 100\%$, where D_s = the diameter of the artery at the site of the most severe stenosis and D_n = the diameter of the distal normal artery (12,13). In the present study, 186 eligible vascular locations were included in Group A and Group B.

Subjective image quality evaluation

All CT images were independently assessed by 2 professional radiologists with 5 years of experience in CTA. CTA image quality was assessed on a 5-point

Table 1 Results of objective image quality analysis

Group	SNR			CNR		
	ICA	MCA	BA	ICA	MCA	BA
A (n=31), mean ± standard deviation	31±22	16±13	12±9	29±21	14±12	11±8
B (n=31), mean ± standard deviation	34±28	16±14	14±14	30±25	14±12	12±12
t value	-0.647	-0.281	-1.010	-0.317	-0.187	0.432
P value	0.520	0.779	0.321	0.752	0.852	0.796

A, CTA-DF-CTP; B, conventional CTA. SNR, signal-to-noise ratio; CNR, contrast-to-noise ratio; ICA, internal carotid artery; MCA, middle cerebral artery; BA, basilar artery; CTA-DF-CTP, computed tomography angiography derived from computed tomography perfusion; CTA, computed tomography angiography.

scale according to image noise, artefact, sharpness, and contrast (14). The scoring criteria were as follows: 5, excellent, neither noise nor artefacts, images with clear and sharp edges, high and homogenous contrast in the lumen; 4, good, low noise, minimal artefacts and blurred edges, good and homogenous contrast; 3, fair, mild graininess or streak artefacts and blurred edges, slightly heterogeneous contrast; 2, poor increased graininess or streak artefacts and blurred edges, heterogeneous contrast, limited diagnostic confidence; 1, unacceptable, obvious graininess or streak artefacts and blurred edges, poor contrast, no diagnostic confidence. Image quality was considered diagnostic at scores from 3 to 5 and non-diagnostic at a score of 1 and 2. In cases where there was disagreement between the 2 radiologists, the score was determined by consensus.

Radiation dose analysis

The CT volume dose index (CTDI_{vol}) and the dose length product (DLP) were used to estimate the radiation dose. The CTDI_{vol} and DLP of each patient were recorded according to the dose report generated by scanner machine. The effective radiation dose (ED) was calculated based on the formula $ED = DLP \times k$, where k is the conversion coefficient, and the value of k in head and neck CTA is 0.0031 (15).

Statistical analysis

Data were analyzed using the software SPSS 26.0 (IBM Corp., Armonk, NY, USA). The results were presented as the mean ± SD. The paired-samples *t*-test was performed to analyze differences in objective image quality (vascular attenuation, image noise, SNR, and CNR) between Groups A and B. The Mann-Whitney *U* test was used to compare image quality scores. The kappa statistic was used to

assess inter-reader agreement in the evaluation of image quality scores in Group A and Group B. Bland-Altman analysis was used to assess agreement in the evaluation of the vascular stenosis rate of Groups A and B. A Bland-Altman scatter plot was drawn to analyze the consistency of the diagnostic vascular stenosis rate in Group A and Group B. The stenosis rate measured on the CTA-DF-CTP image was taken as the standard measurement value, which was taken as the X-axis, and the difference between the stenosis rate measured in Groups A and B was taken as the Y-axis. The limit of agreement (LOA) was the median of the difference (*M*) ± 1.96 SD. The consistency of the two image measurement methods under different bounds was evaluated by the proportion of boundary points.

Results

Objective image quality

There were no significant differences in image noise, SNR, or CNR between the 2 groups ($P > 0.05$) (Table 1); however, the mean vascular attenuation of Group A was higher than that of Group B ($P < 0.01$) (Table 2). Among 186 arteries examined in 31 patients, 43 vessels were diagnosed with varying degrees of stenosis in both Group A and Group B. Bland-Altman analysis showed good consistency between CTA-DF-CTP and conventional CTA in the diagnosis of head and neck artery stenosis rate [95% confidence interval (CI): -5.44, 4.99] (Figures 1-3).

Subjective image quality

The image quality of both groups met the requirements of clinical diagnosis, and the difference was not statistically significant (4.97 ± 0.18 vs. 4.94 ± 0.25) points, $Z = -1.414$,

Table 2 Results of objective image quality analysis

Group	Attention (HU)			Noise (HU)		
	ICA	MCA	BA	ICA	MCA	BA
A (n=31), mean ± standard deviation	548±112	453±118	431±99	25±16	45±28	47±21
B (n=31), mean ± standard deviation	454±85	388±70	360±83	33±85	39±27	44±27
t value	-5.952	4.818	4.214	-7.345	1.896	0.741
P value	<0.01	<0.01	<0.01	0.466	0.063	0.465

A, CTA-DF-CTP; B, conventional CTA. HU, Hounsfield units; ICA, internal carotid artery; MCA, middle cerebral artery; BA, basilar artery; CTA-DF-CTP, computed tomography angiography derived from computed tomography perfusion; CTA, computed tomography angiography.

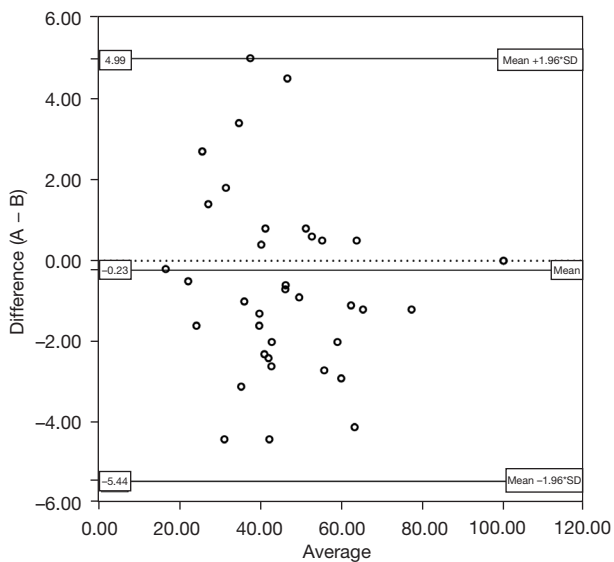


Figure 1 Bland-Altman analysis of arterial stenosis rate. Bland-Altman scatter plot of the diagnostic consistency of the vascular stenosis rate in CTA-DF-CTP and CTA images (n=31). Only 2 cases were outside the consistency limit, and the proportion of data points outside the consistency limit was less than 5%. The two groups of images had good consistency in the diagnosis of arterial stenosis. SD, standard deviation; CTA-DF-CTP, CTA derived from CTP; CTA, computed tomography angiography; CTP, computed tomography perfusion.

$P > 0.05$). There was good agreement between the 2 radiologists in image quality evaluation (kappa value: 0.652, $P < 0.05$) (Figures 4, 5).

Radiation dose

The CTDIvol, DLP, and ED of the CTP scan were

approximately 100.8 mGy, 1,613 mGy·cm, and 5.00 mSv, respectively. The CTDIvol, DLP, and ED of CTA combined with CTP scans were 112.9 mGy, 2,093±88 mGy·cm, and 6.49±0.27 mSv, respectively. Compared with Group B, Group A had 1 fewer CTA scan, and the CTDIvol, DLP, and ED were reduced by 10.7%, 23.0%, and 23.0%, respectively.

Discussion

In this study, we used CTA-DF-CTP to conduct a comprehensive subjective and objective evaluation of the head and neck from the proximal large vessels such as the ICA to the intracranial branch of the MCA and analyzed the stenosis and occlusion of important vessels of the head and neck. Our study found that the quality of CTA images extracted by this method was excellent and the diagnostic efficiency of head and neck artery stenosis was good. Therefore, the CTA scan can be omitted so that patients can reduce the radiation dose and iodine contrast agent injection, which has important clinical implications especially for patients with renal insufficiency. Since conventional CTA is performed at a moment in time, vessels will not be visible if the contrast material has not yet arrived at the time of acquisition. CTA-DF-CTP displays the maximum contrast during the total time of the CTP acquisition. Therefore, it is less susceptible to blurred vascular display resulting from changes in cardiac output or early or delayed arrival due to vascular pathology (16-18).

The present study showed that there were no significant differences in noise, SNR, or CNR between CTA-DF-CTP and conventional CTA, but the vascular attenuation of CTA-DF-CTP was higher than that of conventional CTA. The reason for this discrepancy may be that CTA-DF-CTP shows the highest CT value during the total time of CTP

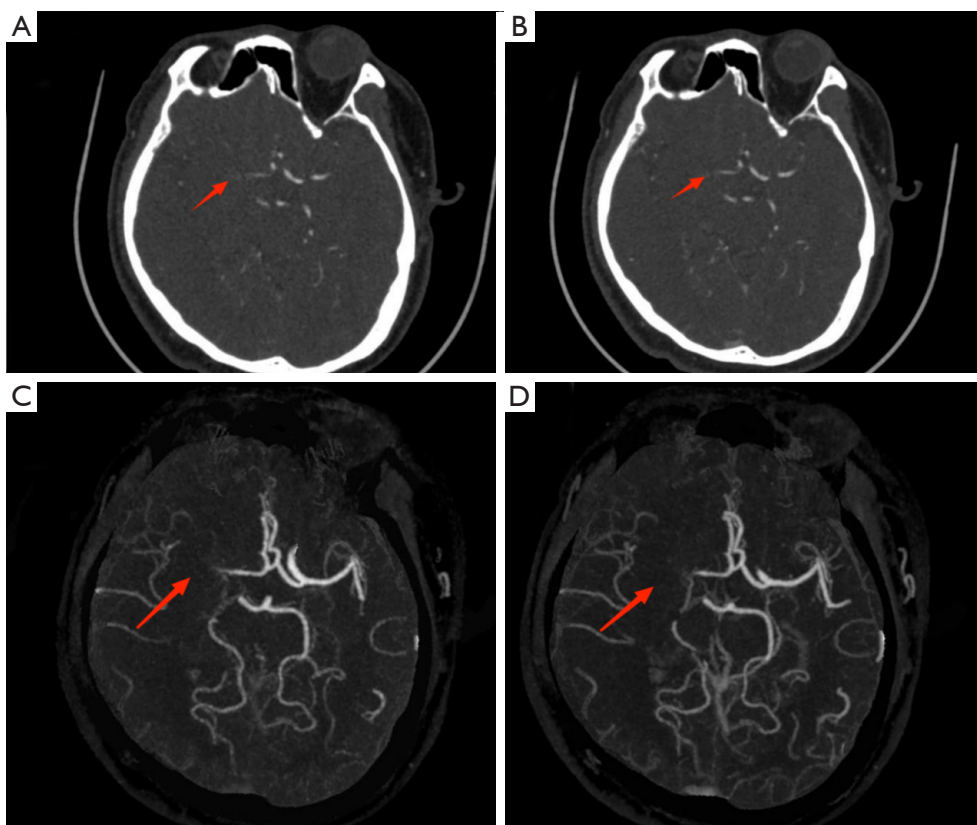


Figure 2 CTA-DF-CTP (A,C) and conventional CTA (B,D) images in a 59-year-old male patient with right middle cerebral artery obstruction. Occlusion of the vessels (red arrows) was detected on both CTA techniques. The slab thickness of MIP was 25 mm. Window settings were kept constant for better comparability (width 1,000 HU, level 300 HU). CTA-DF-CTP, CTA derived from CTP; CTA, computed tomography angiography; CTP, computed tomography perfusion; MIP, maximum intensity projection; HU, Hounsfield units.

acquisition. At the same time, the 2 groups of images had excellent consistency in the diagnosis of vascular stenosis rate. The image quality of CTA-DF-CTP is good enough to provide diagnostic accuracy for the detection of arterial stenosis and occlusion. Therefore, it was unnecessary to perform a separate CTA acquisition of the brain. In addition, for some patients with CTA combined with CTP examination, CTA-DF-CTP can be used to compensate for the failure of CTA scans caused by large image artefacts due to poor patient cooperation or other reasons.

In recent years, with the wide application of CTA, the radiation dose and contrast-induced nephropathy related to CTA examination have attracted great attention from researchers (19,20). In light of the guideline recommendations, CTP is increasingly used in the selection of patients with clinically suspected stroke (21). The American Heart Association (AHA) stroke guidelines specifically recommend CTP imaging to select stroke

patients for endovascular therapy in the 6–24-hour time window and do not recommend the use of CTP imaging in the early time-window (22). However, the current view of some scholars is that the success of endovascular therapy depends on whether patients with significant cerebral tissue at risk can be rescued by reperfusion, irrespective of the strict time window (23). Alexandre *et al.* found that CTP can also be used for large vessels occlusion treated beyond 6 hours from symptom onset (24). However, CTA combined with CTP results in more radiation doses and more contrast agents that expose patients to a higher risk of renal insufficiency. From our study, we can see that if the patient could avoid surplus CTA examination and receive less iodine contrast agent injection, the ED could be decreased by 23.0%, provided that the image quality was guaranteed. CTP protocols vary in different medical CT manufacturers and institutions. In our study, the whole brain CTP scanning covered 160 mm from the skull base

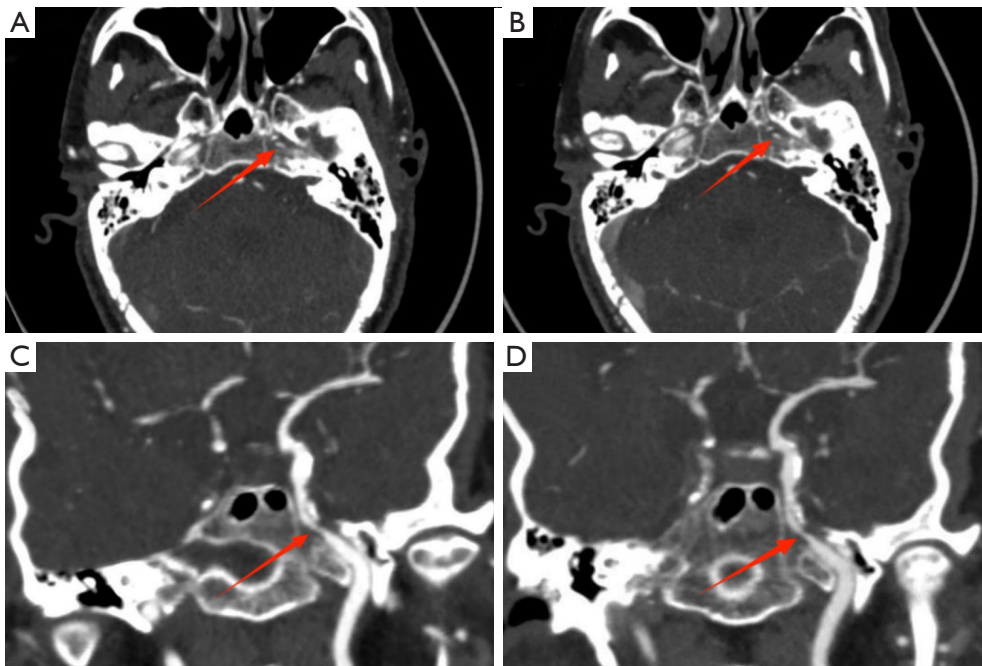


Figure 3 CTA-DF-CTP (A,C) and conventional CTA (B,D) images in a 69-year-old male patient with left internal carotid artery stenosis. Severe stenosis of the vessels (red arrows) was detected on both CTA techniques. Window settings were kept constant for better comparability (width 1,000 HU, level 300 HU). CTA-DF-CTP, CTA derived from CTP; CTA, computed tomography angiography; CTP, computed tomography perfusion; HU, Hounsfield units.

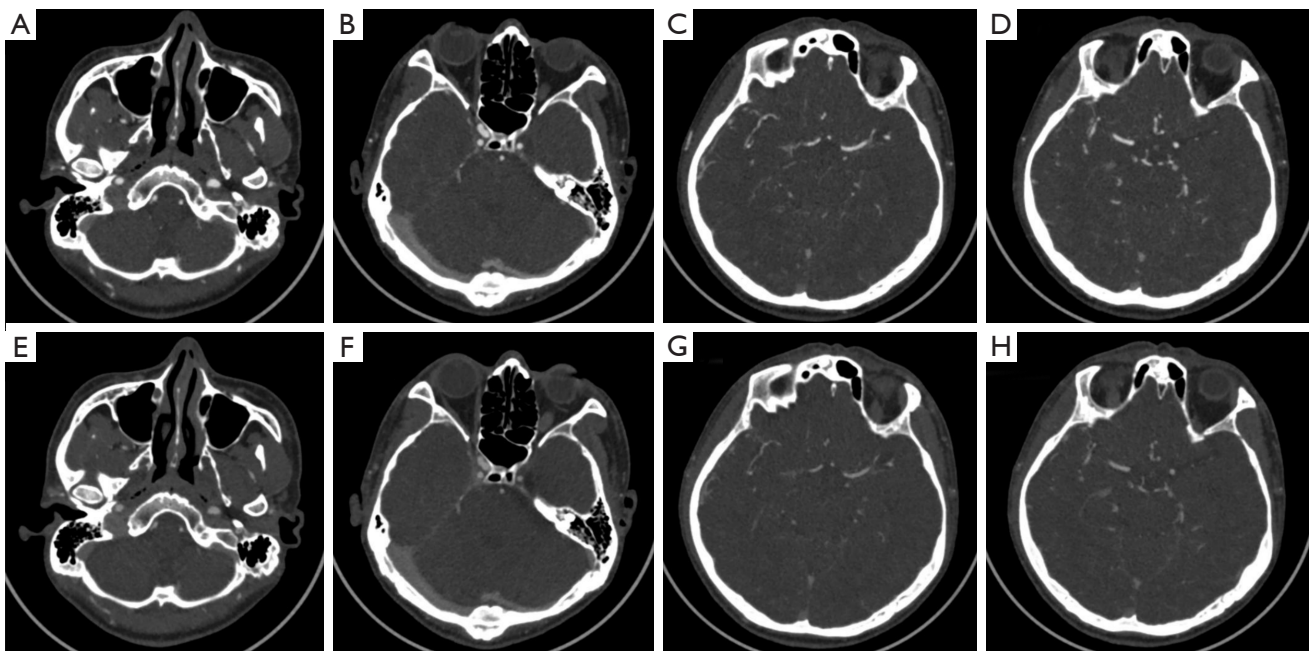


Figure 4 CTA images of a 31-year-old male patient without cerebral artery stenosis or occlusion. (A-D) CTA-DF-CTP images of the bilateral ICA, BA, and bilateral MCA. (E-H) Conventional CTA images of the bilateral ICA, BA and bilateral MCA. Window settings were kept constant for better comparability (width 1,000 HU, level 300 HU). CTA, computed tomography angiography; CTA-DF-CTP, CTA derived from CTP; CTP, computed tomography perfusion; ICA, internal carotid artery; BA, basilar artery; MCA, middle cerebral artery; HU, Hounsfield units.

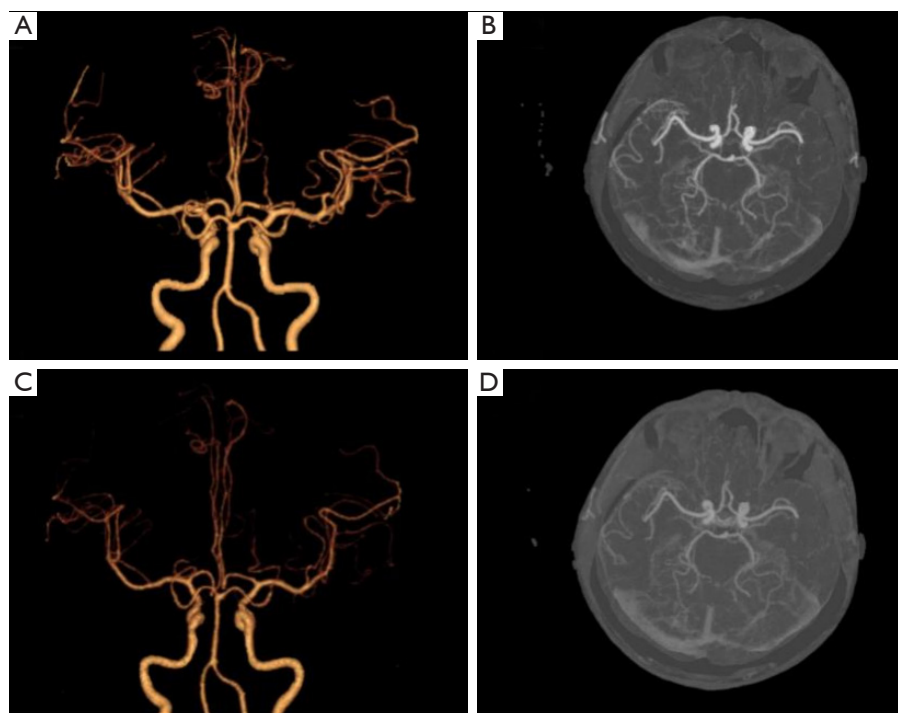


Figure 5 VR and MIP reconstruction images of the 31-year-old male patient in *Figure 4*. (A,B) VR and MIP images of CTA-DF-CTP. (C,D) VR and MIP images of conventional CTA. The slab thickness of MIP was 25 mm. Window settings were kept constant for better comparability (width 1,000 HU, level 300 HU). VR, volume rendering; MIP, maximum intensity projection; CTA-DF-CTP, CTA derived from CTP; CTA, computed tomography angiography; CTP, computed tomography perfusion; HU, Hounsfield units.

to the vertex. Some investigations and medical institutions report a coverage of 80–100 mm, in which more radiation dose can be reduced, but the information related to the reduced scan range is lost in the CTA-DF-CTP.

To date, with the development of image post-processing technology and artificial intelligence, few studies on CTA-DF-CTP have been reported. The use of anatomical information derived from the CTP data had previously been described to assess collateral scores, clot burden, and retrograde filling of vessels (17,25,26). Smit *et al.* reported that temporally filtered time maximum intensity projection (tMIP) CTA data have excellent image quality that is superior to conventional CTA (10). Smit *et al.* confirmed the diagnostic accuracy for the detection of artery occlusions of time-invariant CTA-DF-CTP in acute stroke (16). Frölich *et al.* validated the use of CTA-DF-CTP in proximal local vascular occlusion, such as the ICA, BA, and MCA-M1 segment (25). Limaye *et al.* also demonstrated that CTA-DF-CTP shows excellent correlation in terms of identifying the presence or absence of occlusion of MCA-M2 (26). Verdolotti *et al.* reported

that a new semi-automatic post-processing software allows a simpler and more immediate evaluation of collateral circulation during stroke (27). As these studies mainly focused on the subjective evaluation of CTA-DF-CTP and the diagnostic accuracy of local vascular occlusion, without evaluating image quality from objective evaluation indicators such as CT value, noise, SNR, and CNR, nor quantitative evaluation of the vascular stenosis rate, the quantitative evaluation of diagnostic efficacy and performance was insufficient.

This study had several limitations. First, the number of patients enrolled in this study was limited, and further large-scale studies should be performed to validate the results. Second, because the CTA scanning range is larger than that of the CTP, the relevant information from the aortic arch to the skull base is lost in the CTA-DF-CTP. Third, only CTA examination was omitted in this study, and CTP examination combined with low tube voltage, automatic milliamperage technology, and low iodine contrast agent intake to further reduce the radiation dose and iodine contrast agent intake remains to be further studied.

Conclusions

CTA-DF-CTP is of good quality and has similar diagnostic performance to conventional CTA in terms of cerebral vessel stenosis and occlusion. In this way, the radiation dose and contrast agent kidney damage received by patients can be reduced while maintaining image quality.

Acknowledgments

The authors would like to thank the whole team of the Department of Radiology, The Second Affiliated Hospital of Soochow University for support and numerous fruitful discussions.

Funding: This study was supported by the Project of State Key Laboratory of Radiation Medicine and Protection, Soochow University (No. GZK1202136), “National Tutor System” Training Program for Health Youth Key Talents in Suzhou (No. Qngg2021006), Suzhou Health Talent (No. GSWS2021025), Suzhou Municipal Science and Technology Development Project (No. SKY2022049), “Technological Innovation” Project of CNNC Medical Industry Co., Ltd. (No. ZHYLYB2021006), “Image Medical Star” Project of Suzhou Medical Association (No. 2022YX-M05), Pre-Research Foundation of Second Affiliated Hospital of Soochow University (No. SDFEYBS1904), and the Project of Nuclear Technology Medical Application Supported by Discipline Construction of Second Affiliated Hospital of Soochow University (No. XKTJ-HRC20210010).

Footnote

Conflicts of Interest: All authors have completed the ICMJE uniform disclosure form (available at <https://qims.amegroups.com/article/view/10.21037/qims-22-988/coif>). The authors have no conflicts of interest to declare.

Ethical Statement: The authors are accountable for all aspects of the work in ensuring that questions related to the accuracy or integrity of any part of the work are appropriately investigated and resolved. The study was conducted in accordance with the Declaration of Helsinki (as revised in 2013). The study was approved by institutional ethics committee board of The Second Affiliated Hospital of Soochow University and informed consent was provided by all the patients.

Open Access Statement: This is an Open Access article distributed in accordance with the Creative Commons

Attribution-NonCommercial-NoDerivs 4.0 International License (CC BY-NC-ND 4.0), which permits the non-commercial replication and distribution of the article with the strict proviso that no changes or edits are made and the original work is properly cited (including links to both the formal publication through the relevant DOI and the license). See: <https://creativecommons.org/licenses/by-nc-nd/4.0/>.

References

1. Navia P, Larrea JA, Pardo E, Arce A, Martínez-Zabaleta M, Díez-González N, Murias E, Arráez-Aybar LA, Massó J. Initial experience using the 3MAX cerebral reperfusion catheter in the endovascular treatment of acute ischemic stroke of distal arteries. *J Neurointerv Surg* 2016;8:787-90.
2. Jiang J, Dai J, Cui H. Vitexin reverses the autophagy dysfunction to attenuate MCAO-induced cerebral ischemic stroke via mTOR/Ulk1 pathway. *Biomed Pharmacother* 2018;99:583-90.
3. Lev MH, Farkas J, Rodriguez VR, Schwamm LH, Hunter GJ, Putman CM, Rordorf GA, Buonanno FS, Budzik R, Koroshetz WJ, Gonzalez RG. CT angiography in the rapid triage of patients with hyperacute stroke to intraarterial thrombolysis: accuracy in the detection of large vessel thrombus. *J Comput Assist Tomogr* 2001;25:520-8.
4. Neuhaus V, Große Hokamp N, Abdullayev N, Maus V, Kabbasch C, Mpotsaris A, Maintz D, Borggreffe J. Comparison of virtual monoenergetic and polyenergetic images reconstructed from dual-layer detector CT angiography of the head and neck. *Eur Radiol* 2018;28:1102-10.
5. Ma YC, Chen AQ, Guo F, Yu J, Xu M, Shan DD, Zhang SH. The value of whole-brain CT perfusion imaging combined with dynamic CT angiography in the evaluation of pial collateral circulation with middle cerebral artery occlusion. *Technol Health Care* 2022;30:967-79.
6. Sabarudin A, Subramaniam C, Sun Z. Cerebral CT angiography and CT perfusion in acute stroke detection: a systematic review of diagnostic value. *Quant Imaging Med Surg* 2014;4:282-90.
7. Kloska SP, Nabavi DG, Gaus C, Nam EM, Klotz E, Ringelstein EB, Heindel W. Acute stroke assessment with CT: do we need multimodal evaluation? *Radiology* 2004;233:79-86.
8. Cai W, Hu C, Hu S, Wang X, Gong J, Zhang W, Shi D, Cheng B. Feasibility study of iterative model reconstruction combined with low tube voltage, low iodine load, and low iodine delivery rate in craniocervical CT angiography. *Clin Radiol* 2018;73:217.e1-6.
9. Bernard A, Comby PO, Lemogne B, Haioun K, Ricolfi

- F, Chevallier O, Loffroy R. Deep learning reconstruction versus iterative reconstruction for cardiac CT angiography in a stroke imaging protocol: reduced radiation dose and improved image quality. *Quant Imaging Med Surg* 2021;11:392-401.
10. Smit EJ, Vonken EJ, van der Schaaf IC, Mendrik AM, Dankbaar JW, Horsch AD, van Seeters T, van Ginneken B, Prokop M. Timing-invariant reconstruction for deriving high-quality CT angiographic data from cerebral CT perfusion data. *Radiology* 2012;263:216-25.
 11. Niiniviita H, Kiljunen T, Kulmala J. Comparison of Effective Dose and Image Quality for Newborn Imaging on Seven Commonly Used CT Scanners. *Radiat Prot Dosimetry* 2017;174:510-7.
 12. Huang J, Degnan AJ, Liu Q, Teng Z, Yue CS, Gillard JH, Lu JP. Comparison of NASCET and WASID criteria for the measurement of intracranial stenosis using digital subtraction and computed tomography angiography of the middle cerebral artery. *J Neuroradiol* 2012;39:342-5.
 13. Fox AJ. How to measure carotid stenosis. *Radiology* 1993;186:316-8.
 14. Liu B, Gao S, Chang Z, Wang C, Liu Z, Zheng J. Lower extremity CT angiography at 80 kVp using iterative model reconstruction. *Diagn Interv Imaging* 2018;99:561-8.
 15. Rogers LF. Dose reduction in CT: how low can we go? *AJR Am J Roentgenol* 2002;179:299.
 16. Smit EJ, Vonken EJ, Meijer FJ, Dankbaar JW, Horsch AD, van Ginneken B, Velthuis B, van der Schaaf I, Prokop M. Timing-Invariant CT Angiography Derived from CT Perfusion Imaging in Acute Stroke: A Diagnostic Performance Study. *AJNR Am J Neuroradiol* 2015;36:1834-8.
 17. Frölich AM, Wolff SL, Psychogios MN, Klotz E, Schramm R, Wasser K, Knauth M, Schramm P. Time-resolved assessment of collateral flow using 4D CT angiography in large-vessel occlusion stroke. *Eur Radiol* 2014;24:390-6.
 18. Bae KT. Intravenous contrast medium administration and scan timing at CT: considerations and approaches. *Radiology* 2010;256:32-61.
 19. Clark TJ, Gunn ML. CT Angiography in the Emergency Department: Maximizing Contrast Enhancement and Image Quality While Minimizing Radiation Dose and Contrast Material Volume: Vascular/Interventional Radiology. *Radiographics* 2017;37:1304-5.
 20. Ren H, Zhen Y, Gong Z, Wang C, Chang Z, Zheng J. Feasibility of low-dose contrast media in run-off CT angiography on dual-layer spectral detector CT. *Quant Imaging Med Surg* 2021;11:1796-804.
 21. Donahue J, Wintermark M. Perfusion CT and acute stroke imaging: foundations, applications, and literature review. *J Neuroradiol* 2015;42:21-9.
 22. Powers WJ, Rabinstein AA, Ackerson T, Adeoye OM, Bambakidis NC, Becker K, Biller J, Brown M, Demaerschalk BM, Hoh B, Jauch EC, Kidwell CS, Leslie-Mazwi TM, Ovbiagele B, Scott PA, Sheth KN, Southerland AM, Summers DV, Tirschwell DL. Guidelines for the Early Management of Patients With Acute Ischemic Stroke: 2019 Update to the 2018 Guidelines for the Early Management of Acute Ischemic Stroke: A Guideline for Healthcare Professionals From the American Heart Association/American Stroke Association. *Stroke* 2019;50:e344-418.
 23. Santos T, Carvalho A, Cunha AA, Rodrigues M, Gregório T, Paredes L, Costa H, Roriz JM, Pinho J, Veloso M, Castro S, Barros P, Ribeiro M. NCCT and CTA-based imaging protocol for endovascular treatment selection in late presenting or wake-up strokes. *J Neurointerv Surg* 2019;11:200-3.
 24. Alexandre AM, Pedicelli A, Valente I, Scarcia L, Giubolini F, D'Argento F, Lozupone E, Distefano M, Pilato F, Colosimo C. May endovascular thrombectomy without CT perfusion improve clinical outcome? *Clin Neurol Neurosurg* 2020;198:106207.
 25. Frölich AM, Psychogios MN, Klotz E, Schramm R, Knauth M, Schramm P. Angiographic reconstructions from whole-brain perfusion CT for the detection of large vessel occlusion in acute stroke. *Stroke* 2012;43:97-102.
 26. Limaye K, Bryant A, Bathla G, Dai B, Kasab SA, Shaban A, Samaniego EA, Hasan D, Policeni B, Leira E, Derdeyn C, Ortega-Gutierrez S. Computed Tomography Angiogram Derived From Computed Tomography Perfusion Done with Low Iodine Volume Protocol Preserves Diagnostic Yield for Middle Cerebral Artery-M2 Occlusions. *J Stroke Cerebrovasc Dis* 2019;28:104458.
 27. Verdolotti T, Pilato F, Cottonaro S, Monelli E, Giordano C, Guadalupi P, Benenati M, Ramaglia A, Costantini AM, Alexandre A, Di Iorio R, Colosimo C. ColorViz, a New and Rapid Tool for Assessing Collateral Circulation during Stroke. *Brain Sci* 2020;10:882.

Cite this article as: Zhou XZ, Lu K, Zhai DC, Cui MM, Liu Y, Wang TT, Shi D, Fan GH, Ju SH, Cai W. The image quality and diagnostic performance of CT perfusion-derived CT angiography versus that of conventional CT angiography. *Quant Imaging Med Surg* 2023;13(10):7294-7303. doi: 10.21037/qims-22-988